ACI STRUCTURAL JOURNAL TECHNICAL PAPER

Title no. 103-S03

Tests on Precast Concrete Frames with Connections Constructed Away from Column Faces

by Jyh-Hao Khoo, Bing Li, and Woon-Kwong Yip

A modified assembled configuration is introduced for precast concrete frames in which the connections are constructed on the beam span and kept away from the column faces so as to avoid coinciding with the plastic hinge regions during seismic excitations. An experimental study on the seismic performances of two full-scale precast concrete subframes adopting the aforementioned configuration and a monolithically-cast subframe subjected to quasistatic simulated seismic loading is presented. The variable examined was the connection detail. The performances of the precast concrete frames are evaluated on the basis of ductility, energy dissipation capacity, connection strength, and drift capacity. Based on the test results, the precast concrete frames are capable of matching overall performance of the monolithic connections and thereby providing moment-resisting behavior.

Keywords: ductility; frames; precast concrete; seismic.

INTRODUCTION

Structural systems employing precast concrete elements have proven quite efficient in raising productivity and quality control as well as being cost efficient. In countries such as New Zealand and the U.S., precast concrete systems with various connection details have been widely implemented in the construction of moment-resisting frames to provide adequate earthquake resistance. Nevertheless, the precast concrete industry has not reached its full operating potential due to several problems that have been left unsolved for years. Problems arising from the connections between precast components have become a serious issue confronting the precast concrete industry. Some precast concrete structures have demonstrated failure during earthquakes in the past as a result of inadequate attention to the connection design.

The lack of prescriptive design guidelines has also been an obstruction for the comprehensive use of precast concrete structural systems in the construction industry. Naaman et al.[1] stated that the UBC Code[2] allows considerable freedom in the development of ductile moment-resisting frames but little clarification is given on how the provisions can be applied to precast concrete structures. Design codes in the U.S. generally adopt a requirement of proven reinforced concrete emulation for precast concrete seismic-resistant structures.[3] Confidence in the use of precast concrete frames in regions of high seismicity is ultimately based on laboratory testing for the validation of their performance. There is also a lack of accepted design methods for areas of low to moderate seismicity in which the ductility demand may be lower. It appears to be impractical and uneconomical to provide the same level of seismic resistance for precast concrete frames in low to moderate seismic areas as those in regions of high seismicity.

Current practice in precast concrete frame construction reveals that the connections between precast beams are usually located at the beam-column joint cores; or at the midspan of a beam. Providing connection in the beam-column joint region is apparently unfavorable because it disturbs the continuity of reinforcement. The congested reinforcement details in the joints always create difficulties during the erection stage. Moreover, the beam-column joints can be vulnerable under seismic actions as they are subjected to reverse bending moments and shear forces. The induced shear forces in the joint region can typically be in the order of five times the column shear force.[4] A precast beam is normally seated on the column edges, thus coinciding with the inherent plastic hinging region. This situation would probably be most disadvantageous under seismic actions if the connections are not properly designed for strength and ductility. On the other hand, for frames adopting midspan beam-to-beam connections, Park[5] noted that the precast components of this system can be very heavy and difficult to transport due to their relatively large dimensions. This transportation difficulty would then hinder the choice of precasting the cruciform members for frames with long beams.

French et al.[6,7] had looked into the issue of moving the connections away from the column face. In their research, the connections were relocated to the beam span at a distance away from the column faces. Such a configuration implies that a beam-column joint core with short, protruding beam stubs would be cast as part of the precast column, while the beam spanning in between columns would form another precast member. The connections between these precast components were established through the lapping of hooks at the precast beam ends, which were then encased within cast-in-place concrete. Figure 1 schematically illustrates the aforementioned system. With such a frame configuration, the beam-column joint core, in which the reinforcement details are complicated, can be prefabricated precisely under factory conditions. The reinforcement continuity will further enhance the integrity of the joint and prevent premature failure. Most importantly, the coinciding condition between the inherent plastic hinge locations and the connection regions can be avoided. On the other hand, this system allows precast components with longer horizontal members to be mobilized efficiently.

RESEARCH SIGNIFICANCE

The research is relevant to the use of precast concrete systems for gravity-dominated frames in countries located in

ACI Structural Journal, V. 103, No. 1, January-February 2006.
MS No. 04-087 received March 12, 2004, and reviewed under Institute publication policies. Pertinent discussion including author's closure, if any, will be published in the November-December 2006 *ACI Structural Journal* if the discussion is received by July 1, 2006.

Jyh-Hao Khoo *is a senior engineer in Utraco Structural Systems, Singapore. He received his BEng from Universiti Teknologi Malaysia and MEng from Nanyang Technological University, Singapore. His research interests include prestressing, precasting, structural strengthening, and heavy lifting works.*

ACI member **Bing Li** *is an associate professor in the School of Civil and Environmental Engineering, Nanyang Technological University. He received his PhD from the University of Canterbury, New Zealand. His research interests include reinforced concrete and precast concrete structures, particularly in design for earthquake and blast resistance.*

ACI member **Woon-Kwong Yip** *is an associate professor and Vice Dean of the School of Civil and Environmental Engineering, Nanyang Technological University. His research interests include the microfailure of concrete, confined concrete, and precast concrete structures.*

regions of low to moderate seismicity, where the connections are required to transfer forces originated by shear and bending. This research is significant in providing information on seismic behavior of precast moment-resisting frames with cast-in-place connections located in a region other than at the conventionally located column face or at the midspan of a beam. The experimental results presented herein may be of importance in providing evidence on the structural adequacy and the cast-in-place construction emulation capability of the precast concrete systems.

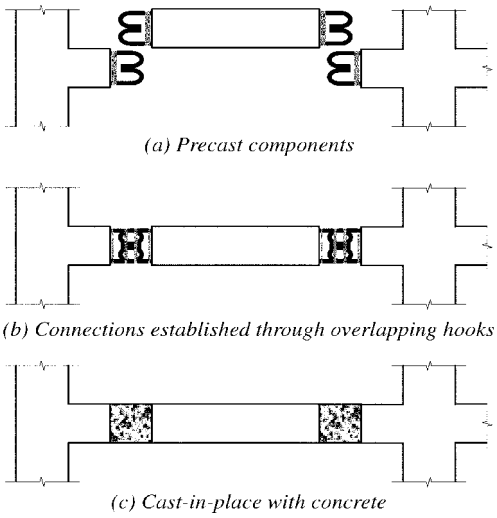

Fig. 1—Precast concrete frame with modified assembling configuration.

DESCRIPTION OF EXPERIMENTAL PROGRAM

Details of test specimens

The emphasis in this experimental program was on the one-way precast concrete beam-column subassemblages typical of a perimeter frame of a multistory building in low to moderate seismic risk zones such as in Singapore and the eastern and central U.S. Three units of test specimens, denoted respectively as Unit 1 to Unit 3, of equal dimensions and reinforcement details as shown in Fig. 2, were constructed and tested to assess the seismic performance and characteristics of the precast beam-column subassemblages described. The connection details examined in this paper were similar to that used by Restrepo et al.;[8,9] they have reported results of earlier tests on similar connection types, but the connection was constructed at beam midspan. The specimens were full-scale prototype subassemblages incorporating exterior beam-column joints and formed an H-shaped structure. These frames were restricted to the category of frames with limited ductility. According to the NZS 3101,[10] for structures of limited ductility, the capacity design procedures are not compulsory and less rigorous detailing requirements are specified, provided that certain strength enhancement requirements are upheld. In this study, the code requirements for limited ductile detailing were generally followed, except that in the joint cores, the horizontal and vertical shear reinforcement provided was only approximately 30% of that required by the NSZ 3101[10] code.

The variable in these specimens was the connecting detail between beams. Unit 1 was cast monolithically to serve as the control specimen. The connections for Unit 2 were composed of overlapping 90-degree hooks. All the beam longitudinal bars were spliced using such hooks and the overlaps started at about 1.8*d* from the column face, where *d* is the effective beam depth. Two sets of stirrups spaced at 120 mm were installed at the overlapping hooks. The connection of Unit 3 consisted of overlapping 180-degree hooks starting at 1.75*d* from the column face. Unit 3 also had two sets of stirrups spaced at 120 mm in the connection regions.

All the frames were envisaged to achieve a beam side-sway mechanism when subjected to earthquake-type loading and to attain the strong column-weak beam behavior. In accordance with that, the ratio of the calculated column-to-beam flexural strengths was, on average, 1.86 for all the test specimens. The flexural strength was calculated based on the

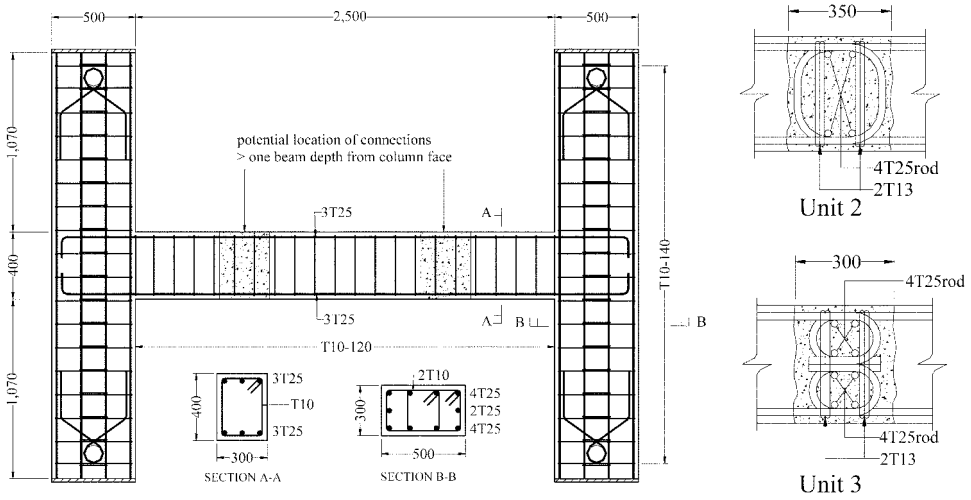

Fig. 2—Typical dimensions and reinforcement details of specimens.

Fig. 3—View of test setup.

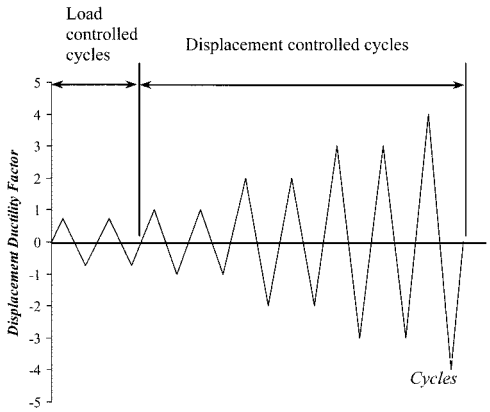

Fig. 4—Quasistatic test sequence used for tests.

strain compatibility-equilibrium approach, the measured stress-strain relationship for steel and an equivalent rectangular stress block for concrete and assuming that the plane section remains plane.

Specimen construction

Commercial premixed concrete (f_c' = 60 MPa) was used in all the casting of the test specimens. The maximum specified aggregate size was 20 mm. All the longitudinal and transverse reinforcements used for the test specimens were high-yield-strength bars of Grade 460 (f_y = 460 MPa). T25 (deformed bar with 25 mm nominal diameter) bars were used for the longitudinal reinforcements while T13 and T10 bars formed the transverse reinforcement. For convenience, the specimens were assembled in the horizontal plane and lifted up to the vertical plane for testing.

Loading arrangement

All the test specimens were loaded under quasistatic simulated seismic loading. A set of loading frames that was previously designed by Restrepo[9,10] was adopted in this study. With such a configuration (Fig. 3), equal lateral displacements could be applied simultaneously to both of the columns of the test specimens so as to induce a bending moment to that generated in the beams under earthquake conditions. To displace both columns simultaneously, an upward displacement was applied to the double-acting hydraulic jack at one side while a downward displacement was applied to another jack at the opposite side. The directions of these two jacks were inter-reversed to generate a load reversal so as to simulate the effects of earthquake-induced lateral forces on a frame.

The specimens were subjected to cyclic reversals of inelastic displacement following recommendations made by Park,[11] as that illustrated in Fig. 4. The first two loading cycles were controlled with load increments within the elastic range. In these cycles, the specimens were quasistatically loaded to $\pm 0.75P_{th}$, where P_{th} is the theoretical total lateral load capacity of the specimens calculated using the measured material properties and assuming an equivalent rectangular stress block for compressed concrete and a bilinear stress-strain relationship for steel bars. The corresponding positive and negative lateral displacements measured at the column tops at the peak of these two cycles were averaged. The obtained value was the displacement at $\Delta_{0.75}$, which correlated with the application of load at $0.75P_{th}$. Consequently, the initial yield displacement Δ_y was linearly extrapolated as $\Delta_{0.75}/0.75$. Displacement-controlled cycles were applied from the third cycles onward in terms of displacement ductility factors μ_Δ, which is defined as Δ/Δ_y, where Δ is the imposed lateral displacement.

Instrumentation

The test specimens had been extensively installed or mounted with measuring devices both internally and externally. Two units of electrical resistance strain gauge load cells, one at each side, were used to determine the applied load from the hydraulic jacks. The lateral displacement at the top of the columns was measured using displacement transducers, which were supported on steel frames fixed directly onto the floor. A range of displacement transducers was also placed along the beam-ends and connection regions to estimate the flexural and shear deformations. On the other hand, electrical resistance strain gauges were used to measure the local strains in the reinforcement during load reversals.

DESCRIPTION OF TEST BEHAVIOR

The general behavior of the tested specimen was identified based essentially on the visible crack patterns, the load-displacement hysteretic responses, and the local strains observed in the reinforcement. All test results described herein are in correspondence with the imposed displacement ductility factors expressed in an abbreviated form, for example, ±DF of 1. The positive and negative signs indicate the directions of the loading cycles while DF of 1 stands for a displacement ductility factor of 1.

Figure 5 illustrates the observed crack patterns in each test specimens at different ductility levels during the test. The painted portions in Units 2 and 3 indicate the connection regions. The reversed cyclic performance is reflected through load-displacement hysteresis loops shown in Fig. 6. The lateral loads shown in the figures are the summation of loads applied to both columns, which is also the total induced story shear. The estimated theoretical lateral load, P_{th} is also indicated. Figure 7 exhibits the tensile strain profiles for the beam bottom longitudinal bars, measured at the peak displacements of each ductility level.

Unit 1 (control specimen)

In the loading cycles into ±DF of 0.75, several flexural tension cracks were initiated along the top and bottom chords of the beam-ends. Flexural shear cracks became apparent when the test progressed into loading cycles of ±DF

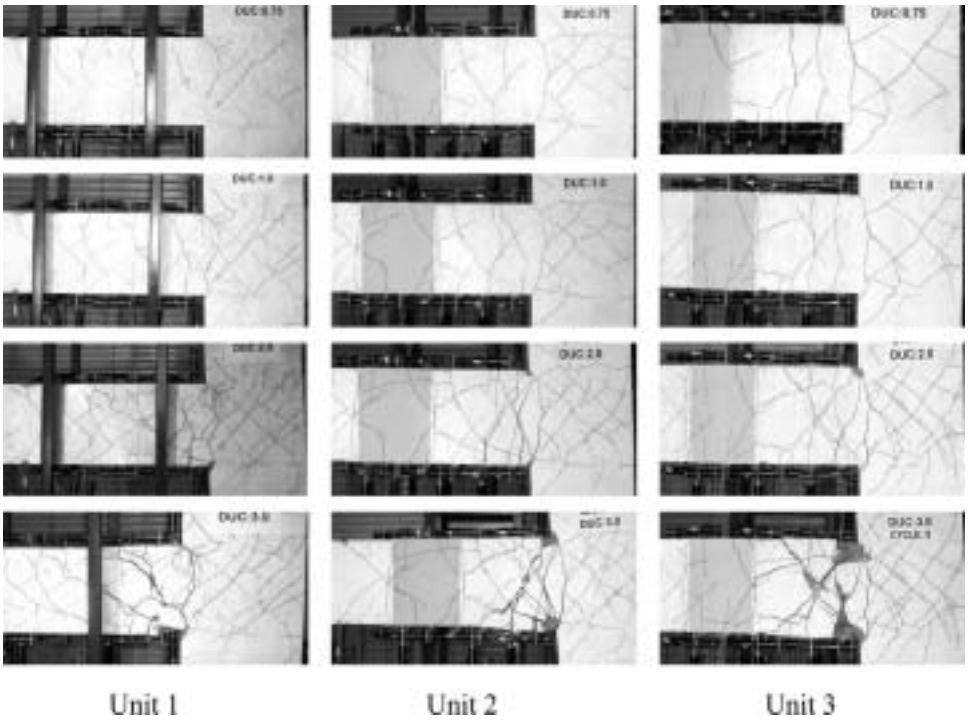

Fig. 5—Crack patterns of specimens at different stages during test.

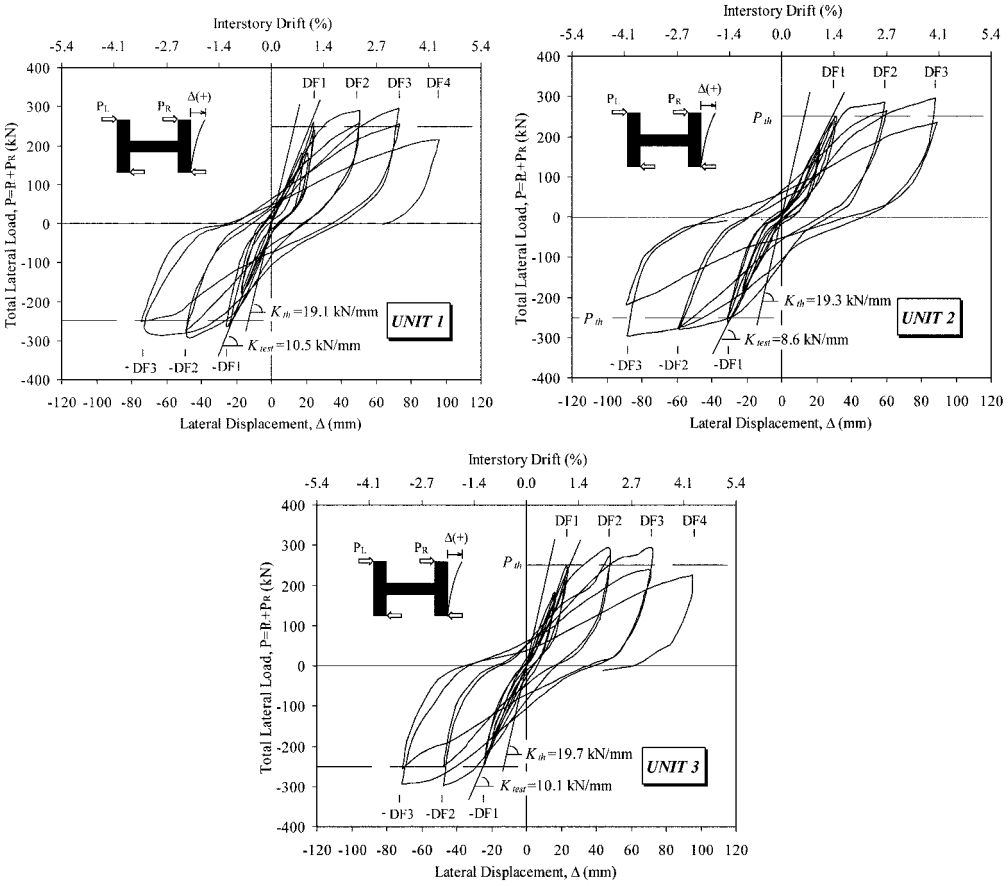

Fig. 6—Lateral load-displacement responses of specimens.

of 1 and kept propagating in a diagonal direction toward the column faces. In the beam-column joint cores, corner-to-corner diagonal tension cracks were found. It was apparent that the diagonal strut and the panel truss actions had been developed for shear resistance in the joints. Also observed in the beam-column joint cores were bond-splitting cracks initiated from the beam-column interface, and extended aligning with the beam longitudinal bars. Generally, all

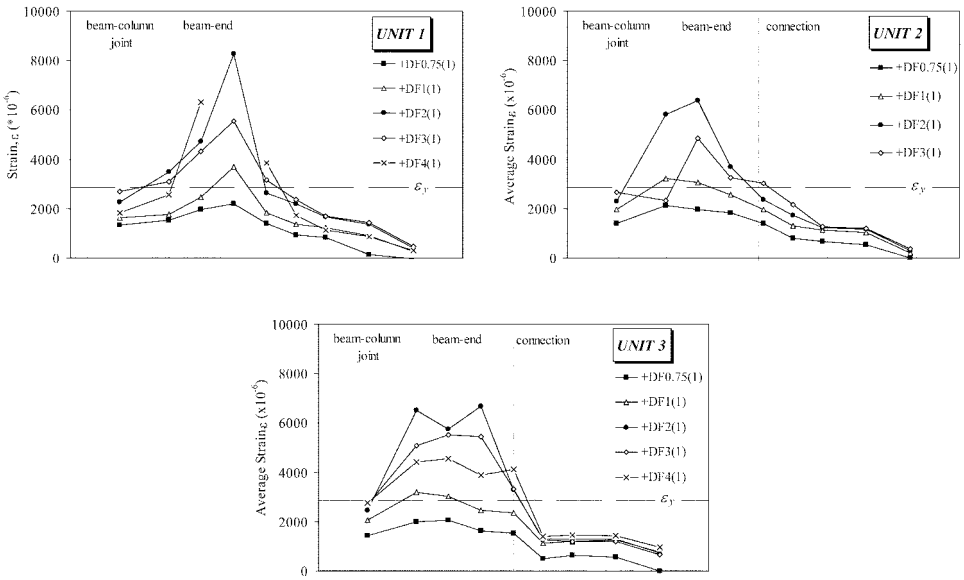

Fig. 7—Local strains in beam bottom bars of specimens.

cracks found during the elastic loading cycles (±DF of 0.75, ±DF of 1) did not widen. As shown in Fig. 6, the measured initial stiffness for Unit 1 was 10.5 kN/mm.

In the post-elastic loading cycles (±DF of 2 onward), more cracks in the beam-web propagated toward the compression zones of the beam-column interface to form a typical fan-shaped pattern. At this stage, it was deemed that a series of concrete struts had completely formed in the beam-end regions to develop a truss-liked action that provided the post-cracked strength and stiffness of the frame. In the first cycle toward ±DF of 2, the hysteresis loop showed obvious signs of bar yielding immediately after surpassing the theoretical lateral load capacity P_{th}, whereby the loop flattens dramatically. This reveals an accurate prediction of the P_{th} value. With reference to the strain profiles for Unit 1 in Fig. 7, yielding of the longitudinal bars spread over a distance of approximately 1.4*d* from the column face, thus indicating the concentration of plastic hinges in the vicinity of this region. The largest tensile strain was detected at 0.92*d* from the column face, which was in the order of $2.95\varepsilon_y$, where ε_y is the yield strain of the bar; however, bars in the beam-column joint had never exceeded the elastic limit. It could thus be concluded that the plastic hinges were successfully confined to the beam end. This was proved by the unopened cracks elsewhere in the beam-column joint cores as the test continued in the post-elastic loading cycles.

Unit 1 exhibited severe deterioration in the plastic hinge regions during the loading cycles into ±DF of 3. Cracks within these regions became wider, and previously opened cracks did not close in the reversed loading runs, resulting in the lengthening of the beam. Crushing of concrete was visible at the corners of the beam-column interfaces. Shear deformations began to dominate the plastic hinge regions whereby enlarged diagonal cracks were observed. The hysteresis loops in the loading cycles at ±DF of 3 became more pinched and showed greater stiffness degradation as well as a loss in the energy dissipation capacity. Nonetheless, the recorded tensile strains in the bars at this stage were much smaller than those measured in ±DF of 2. This could be attributed to severe cracking and shearing of the concrete in the plastic hinge regions, which had caused the loss of bonding between the reinforcement and the concrete and therefore resulted in bar slippage and mobilization of forces in the reinforcement.

As the test proceeded toward ±DF of 4, Unit 1 experienced remarkable strength deterioration and stiffness degradation due to excessive shear deformations. A reduction of 27.2% of lateral load capacity was recorded, implying the hypothetical failure of the frame.

Unit 2 (with overlapping 90-degree hooked connections)

In the elastic loading cycles (±DF of 0.75 and ±DF of 1), the formation and development of cracks were typical of those observed in Unit 1; however, there were vertical cracks along the construction joint between the precast concrete members and the connections. Also appearing in the connection regions were the diagonal cracks at the corners where the bend of the 90-degree hooks took place. These cracks were identified as the bond splitting cracks. More cracks were found in the connection regions as the test progressed into ±DF of 1. The initial stiffness of Unit 2 was less than that of Unit 1 and only accounted for 8.6 kN/mm.

When the unit was loaded to ±DF of 2, the cracks at the beam-end regions widened whereas cracks elsewhere, including those in the connection regions, remained unopened, indicating that a plastic hinge could still develop at the beam-end despite the existence of a connection in the vicinity. With reference to Fig. 7, yielding of reinforcement in Unit 2 spread from the column face to a distance almost equal to the effective depth of the beam *d* and a peak strain of $2.24\varepsilon_y$ was detected at 0.46*d* from the column face. Up to ±DF of 2, there was no sign of yielding penetration into the connection regions; however, the bond-splitting cracks in the connections became denser and extended beyond the construction joints.

At ±DF of 3, the major deformation mode in the beam was governed by shear, as indicated by the enlarged diagonal cracks in the beam-end regions. However, cracks in the connection regions were rather stable. As can be seen in Fig. 6 for Unit 2, the loss of lateral load capacity and the pinching of the hysteresis loops were very significant, as a result of

greater beam shear deformation. In general, Unit 2 had a greater energy dissipating capacity, as indicated by a larger area enclosed by the loops. This could be attributed to the discontinued reinforcement details in the connection regions, which had led to a denser cracking and helped dissipate energy. The measured lateral load in the second cycle reached only 74% of the maximum load previously recorded. Hence, the test was terminated at this stage and the specimen was considered to have failed.

Figure 8 presents stresses along the longitudinal bars in the connection of Units 2 and 3. These stresses were estimated using the measured bar strain profiles and the tested stress-strain relationship for steel. It can be seen that some transfer of forces occurred between the bars at the overlapping regions. It is notable, however, that less stresses in tension were being transferred as the test progressed, probably due to the development of cracks in the connection region and the incipient bond deterioration. The longitudinal bars in the connection region behaved in an elastic manner during the test, but the intrusion of bar yielding occurred at the final stage of the test.

Unit 3 (with overlapping 180-degree hooked connections)

Concrete cracking in this unit showed a similar pattern as that observed in the previous two units. Cracks in the connection region of Unit 3, however, were less than those in Unit 2, possibly because of the improved steel anchorage with the provision of 180-degree hooks in the connections. The initial elastic stiffness of this unit was 10.1 kN/mm, which was almost equivalent to that measured in the control specimen. As the frame was loaded into the inelastic cycle, ±DF of 2, excessive cracking in the beam-end regions developed in association with the yielding of the longitudinal bars. The tensile strain distribution in the bar was rather uniform throughout the region between the column face and the connection face, with an average strain of $2.18\varepsilon_y$ being recorded. Similar to Unit 2, the inelastic tensile strain at the column face was considerably larger. As shown in Fig. 6 for Unit 3, pinching of the hysteresis loops started in the second cycle of ±DF of 2, when shear deformation in the beam appeared to be obvious.

Up to ±DF of 2, cracks in the connection regions had neither increased nor widened, revealing that the stiffness degradation of the frame was mainly due to deformations in the plastic hinge regions. It is also interesting to note that the diagonal cracks initiated in the middle span of the beam did not propagate through the connections. The reinforcement details in the connections were likely to have blocked the propagation of cracks. As shown in Fig. 8 for Unit 3, it appears that there was a transfer of forces between the overlapping bars in the connection region; in fact, the tensile stresses at the intermediate section of the two splices were almost equal. It was believed, however, that force transfer was not through a lapping action because of the short overlapping length. This might also have been due to the anchorage capacity of the 180-degree hooks.

It was evident that beam shear became the dominating failure mode during the loading cycles into ±DF of 3, as shown by the major diagonal cracks in the beam-end region of Unit 3 in Fig. 5. In association with this shear deformation was the bond deterioration in the beam longitudinal reinforcement. Nevertheless, up to this stage, the connections were observed to have no detrimental effect upon the general cyclic

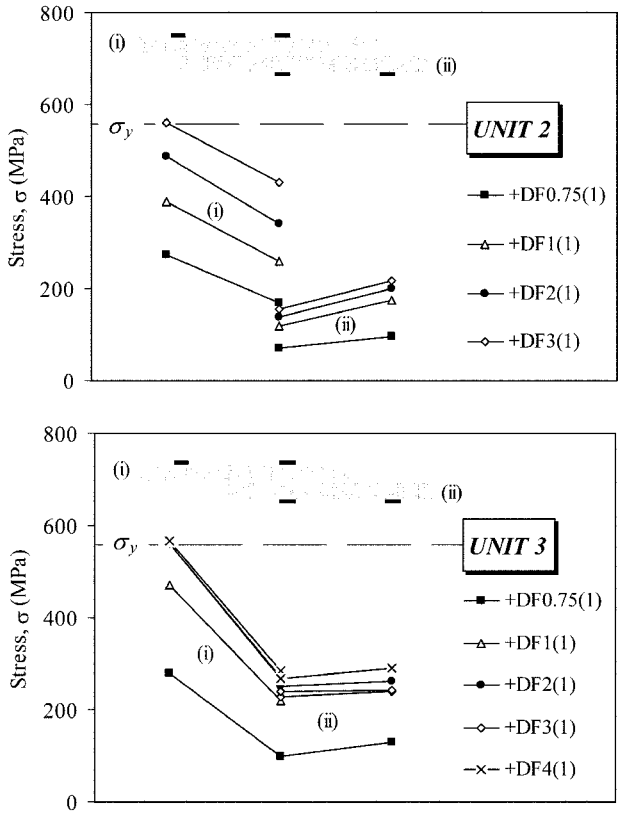

Fig. 8—Stresses in beam longitudinal bars at connection of Units 2 and 3.

performance of Unit 3. The loading run to the first cycle of ±DF of 4 exhibited tremendous stiffness degradation, which was undoubtedly caused by slippage of the longitudinal reinforcement in the plastic hinge regions after large pieces of the concrete cover fell apart. The peak lateral load attained in this load run was only 78% of the maximum recorded value, leading to the end of the test. In general, Unit 3 performed in a manner almost identical to Unit 1 in terms of the load-displacement hysteretic response and energy dissipation characteristics.

DISCUSSION OF TEST RESULTS

Initial stiffness and lateral load capacity

It has been discussed that the initial stiffness of the subassemblages can be evaluated from the application of the first two loading cycles in the elastic range. In fact, the initial stiffness of each subassemblage had been predicted prior to the test based on an elastic analysis using the gross section properties of the columns and beams. To account for cracking in the beams and columns, only half of the gross section properties for flexure and shear were considered. Therefore, the effective moment of inertia was taken as $0.5I_g$ where I_g is the moment of inertia based on an uncracked gross concrete area.

It was found, however, that the stiffness evaluated from the measured lateral displacement was much lower than that theoretically predicted, whereby on average, the difference was approximately 50.4%, as can be seen in Fig. 6. This can be attributed to the large fixed-end rotation in the beam as a result of the penetration of strain in the longitudinal bars into the beam-column joint region. Such a deformation, in fact, contributed to a high percent of decomposition of the total

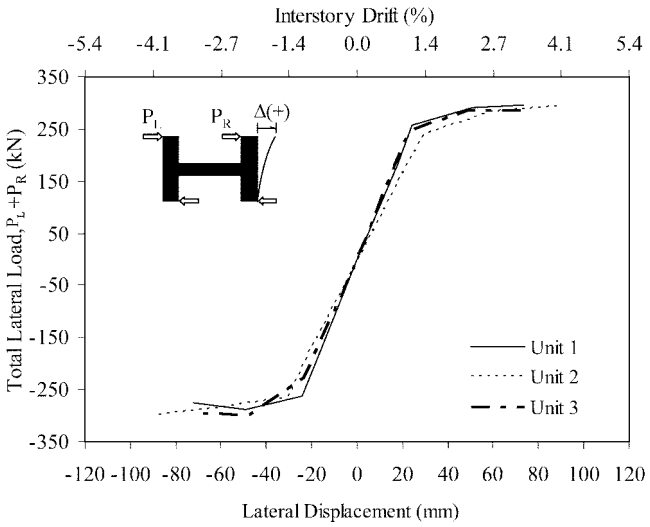

Fig. 9—Load-displacement envelopes of specimens.

Table 1—Positive and negative overstrength

	Theoretical lateral load P_{th}, kN	Positive overstrength		Negative overstrength	
		Maximum load, kN	Increment, %	Maximum load, kN	Increment, %
Unit 1	249.5	295.5	18.4	287.0	15.0
Unit 2	250.0	292.1	16.8	295.5	18.2
Unit 3	250.7	286.8	14.4	298.2	18.9

lateral displacement. However, that was ignored in the calculation of the theoretical stiffness. It is recommended that smaller stiffness values should be considered in the design of moment-resisting frames for earthquake resistance, so that the actual interstory drift would not be underestimated. Figure 9 shows the comparison between the load-displacement envelopes of the precast concrete subassemblages and the control specimen. It is evident that Unit 3, the precast unit connected with 180-degree hooks, showed a nearly perfect correlation to the cast-in-place specimen in terms of stiffness and strength. In contrast, Unit 2 could not attain the initial stiffness comparable to that of Unit 1, but a level of strength similar to that of Unit 1 was gradually developed. The stiffness measured in the test of Unit 2 was approximately 18% less, as a result of premature bonding deterioration in the connections. As reflected by the lateral load-displacement responses, the maximum lateral load attained by each subassemblage exceeded its respective theoretical lateral load calculated from the measured material properties. The flexural overstrength of each test unit for both loading directions is listed in Table 1. Because the measured yield strength of steel was adopted in the prediction of theoretical lateral load capacity, the overstrength due to the variability of actual yield strength above the specified nominal value, which is specified as an overstrength factor in the design code, was unlikely. Therefore, the beam flexural overstrength is mainly because of strength enhancement due to the strain-hardening effect of the reinforcement. The average beam flexural overstrength measured in the tests was $1.17P_{th}$, where P_{th} is the theoretical total lateral load. As recommended in NZS 3101,[8] the overstrength factor should be taken as 1.25 to allow for strain hardening and the actual yield strength being greater than the characteristic yield value.

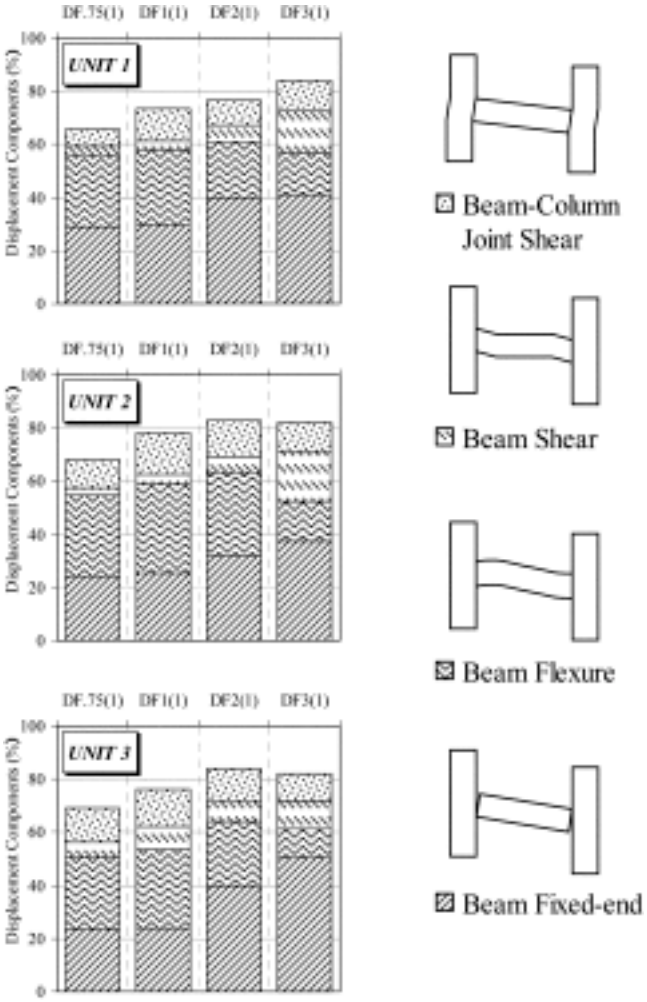

Fig. 10—Member contribution to interstory drift of specimens.

Decomposition of interstory drift

The total interstory drift recorded at the top of the columns consisted of several components. The major components comprised lateral displacements due to the beam fixed-end rotation, beam flexural and beam shear deformation as well as the beam-column joint shear distortion. Data captured by LDVTs mounted on the specimens were used to derive the different sources of deformations, following the procedures described by Restrepo et al.[8,9] Figure 10 presents the contribution of interstory drift components at each ductility level for all the test units. In general, the total calculated lateral displacements due to the contributing components were less than the measured interstory drift. The uncounted lateral displacement could mainly be attributed to the rigid body rotation, which was unable to be captured during the test. Column deformation might have contributed, but it was comparatively insignificant throughout the test. During the loading cycles in the elastic range, ±DF of 0.75 and ±DF of 1, the fixed-end rotation at the column face and the flexural deformation in the beam-end were the major sources of lateral displacement, both of which contributed in total more than 50% of the interstory drift. This conformed to the visible crack patterns on the test units, in which the flexural tension cracks in the beam and the vertical cracks along the beam-column interfaces are the dominating cracks. In the elastic range, displacement due to shear deformation in the beam was relatively insignificant compared to the shear

deformation in the beam-column joint. This could be verified by the denser distribution of diagonal cracks in the beam-column joint cores compared to that at the beam-ends. As the test proceeded to the inelastic range, ±DF of 2 and ±DF of 3, the beam fixed-end rotation became very significant due to the strain penetration of the beam longitudinal reinforcement into the beam-column joint. By contrast, it is interesting to note that the contribution due to flexural displacement in the beam gradually decreased as the test progressed. Instead, lateral displacement due to beam shear had a notable increase, whereby a contribution of approximately 15% of the interstory drift was recorded at the end of the tests. This was credited to the large shear deformations in the plastic hinge regions, in which the beam section tended to slide along the interconnected cracks. The distribution trend shown by the beam flexure and beam shear obviously indicated a deterioration mode when a beam was subjected to a combined flexure and shear force. On the other hand, shear deformation in the beam-column joint also contributed quite significantly but it was still relatively small throughout the test. It is also notable that shear deformation in the beam-column joint gradually reduced in the inelastic loading cycles after the plastic hinges at the beam-ends had fully developed to confine the major deformations. The precast units and the completely cast-in-place unit had shown a rather similar trend in the decomposition of interstory drift. Conforming to the greater interstory drift recorded for Unit 2, the beam flexure deformation in this unit was the greatest among all units. It is believed that the premature bond deterioration in the beam-to-beam connections of this unit had imposed a certain degree of rotation to the beam.

Tensile strain distribution in plastic hinge regions

The profiles demonstrating tensile strains in the beam bottom longitudinal reinforcement at different ductility levels of the three tested specimens are plotted in Fig. 7. These figures show the distribution of tensile strains in the beam plastic hinge region, the beam-to-beam connection region as well as in beam-column joint. It is noticeable that the strain distribution trend for the precast units (Units 2 and 3), in both the elastic and inelastic loading cycles, were quite distinguishable from those shown in the cast-in-place unit (Unit 1). Since the beginning of the tests, the tensile strains in the beam longitudinal reinforcement of Unit 1 spread with a smaller value and peaked at a distance of about d from the column face, where d is the effective beam depth. The maximum inelastic tensile strain in the plastic hinge region was detected at $0.92d$ from the column face, on the order of $2.95\varepsilon_y$, where ε_y is the yield strain of the reinforcement. The maximum tensile strain at the column face was only $1.23\varepsilon_y$. It is evident that for a longer-spanning beam of a frame, for example, a beam with a span-depth ratio of 6.25 as in this test, the critical section in a plastic hinge may not be developed immediately at the column face.

The tensile strains recorded for both the precast units in both the elastic and inelastic cycles, however, spread quite evenly along the beam-end region, within a distance of d from the column face. The average inelastic strain in ±DF of 3 was $2.24\varepsilon_y$; however, it is notable that the steel reinforcement at the column face sustained a greater strain compared to that of Unit 1. It is believed that the greater percentage of steel area in the beam-to-beam connections as a result of essential splicing details had enabled the section to develop greater flexural rigidity, EI, compared to other sections in the proximity, thus sustaining less strain. This might have increased the tendency of greater strain values at the column face.

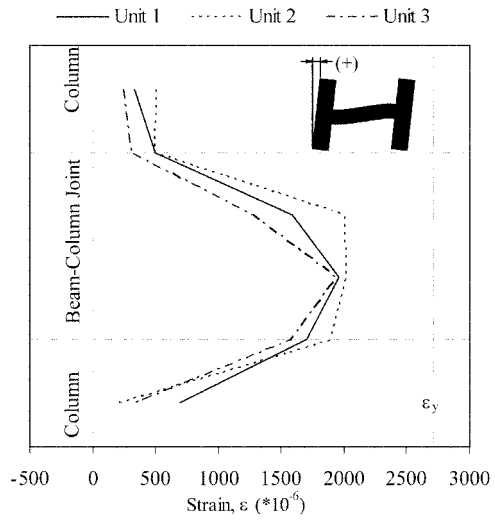

Fig. 11—Comparison of joint hoop strains for specimens.

Nevertheless, it can be confirmed that yielding did not penetrate into the far end of the reinforcement in the beam-column joints in all the tested specimens, as proven by the recorded tensile strains being smaller than the yield strain. It is believed that the use of high-strength concrete ($f_c' = 60$ MPa) had aided the preservation of bond strength between the steel bars and the concrete in the beam-column joints, so that the effective development length for the anchorage could always be available to absorb the yield strength of the bar.

Strains in transverse reinforcement of beam-column joint

The tensile strain profiles of the transverse reinforcement in the beam-column joint at ±DF of 3 for all units are shown in Fig. 11. It is evident that the transverse reinforcement showed no sign of yielding throughout the test. This explained why the cracks observed in the beam-column joint core did not widen throughout the test. The maximum recorded tensile strain was only $0.73\varepsilon_y$. In general, the strain profiles show a typical arch shape against the height. The strains measured in the rectangular ties placed in the column were much smaller than ties placed inside the joint. Such a distribution trend implied that the shear force applied to a beam-column joint is larger than elsewhere in the column. According to Lin et al.,[4] the input shear force in the joint region is typically on the order of five times the column shear force. This statement can be verified by the illustrated strain profiles in which the difference is also about five times. The strain profiles so shown are also in agreement with the observed cracking patterns whereby many diagonal tension cracks were found in the beam-column joint panel compared to the column. In general, the connection details in the beam-to-beam connections did not affect the performance of the beam-column joints under reversed cyclic loading. In fact, the precast frames so connected would yield a straightforward design for the beam-column joints subjected to earthquake loading.

Effects of overlapping 90- and 180-degree hooked connections

The beam-to-beam connections in Units 2 and 3 were established using 90- and 180-degree hooks, respectively.

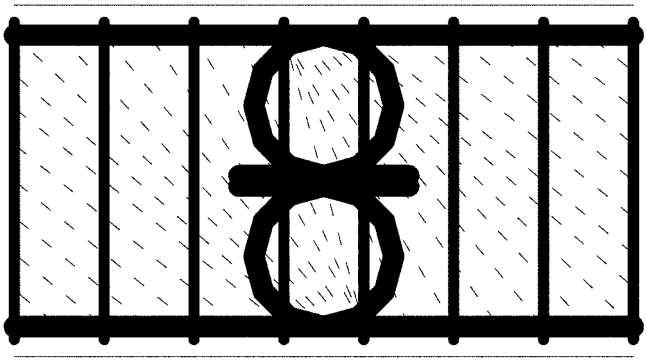

Fig. 12—Compressive stress fields in connection region.

To minimize the length of the cast-in-place connection of a beam, the provision of hooked bar anchorage is necessary to enable the development of full strength in a bar and to ensure a transfer of forces with that bar. As can be seen in Fig. 2, the overlapping length for the straight portion of the hooked bars in the connections is too short and therefore ineffective in transferring forces through a lapping action.

As illustrated in Fig. 5, extensive cracks were observed in the connections of Unit 2 at an early stage of the test. These cracks were identified as the bond splitting cracks. When the tension force is induced in the longitudinal bars, stresses will be generated along the bend and transferred rapidly into the concrete. The anchorage of a bar is established by means of bearing against the concrete and through the frictional bond stresses around the concave side of the bend. The radial components of the stresses acting on the concrete in contact with the bar will exert a pressure on the circumferential surface of the concrete, which will be equilibrated by a so-called circumferential tensile stress in the concrete. Concrete splitting along the bend, as shown by the diagonal cracks in the connections, will occur when the tensile strength of the concrete is exceeded. It is believed that these premature splitting cracks had resulted in a significant local deformation in the connection itself and led to a reduced initial stiffness, as observed in the test of Unit 2.

Apart from that, one should recognize that a bend introduces stress concentration in the concrete in contact with the concave side of the bend. Figure 12 illustrates a truss model for a connection detail involving overlapping hooks. Because there is no continuity between the overlapping hooked bars, the whole beam shear has to be locally transferred by a tension tie between the top and bottom bars. The resulting diagonal compressive stress field will concentrate at the bend and this will also increase the tendency of splitting in the concrete.

With reference to Fig. 5, it is evident that the 180-degree hooks had provided anchorage superior to the 90-degree hooks under the effect of load reversals due to the provision of sufficiently embedded length. The cracks originated at the bend of the 180-degree hooks were less and did not penetrate as the loading progressed. Another favorable observation for Unit 3 was that the connections were free from bond splitting cracks along the straight portion of the hooked bars until the frame was displaced to a large displacement. Such a satisfactory anchorage condition had aided the development of strength within the bars in the plastic hinge regions, and thus resulted in a greater attainable strength and stiffness compared to Unit 2.

Significant beam elongation issue

Beam elongation became apparent in the inelastic loading cycles during the tests of all the specimens. The elongation could be estimated by measuring the horizontal displacement at the pin support of the free-to-slide mechanism in the test frame. Measured beam elongation in these tests was approximately 50 mm. The primary source for the beam elongation was the residual inelastic tensile strain in the longitudinal reinforcement of the beam. For beams with equal amounts of top and bottom reinforcement, the elongation of the bars tended to accumulate during reserved cyclic loading because the compression reinforcement in the plastic hinge regions retained a significant tensile strain from its previous state when it had been in tension.

CONCLUSIONS

Quasistatic reversed cyclic loading experiments were conducted on two types of precast concrete subframe systems and their monolithic counterpart. From this study, the following conclusions can be drawn:

1. It is evident that the modified precast frame configuration with relocated beam-to-beam connections is feasible as a replication of cast-in-place moment-resisting frames. The "strong connection" approach adopted in this study is of particular importance in achieving the elastic behavior of the connections so as to allow for the development of yield strength in the reinforcement at the plastic hinge regions. The modified precast frame had allowed for the formation of plastic hinges in the beam-end regions and within the proximity of about an effective beam depth d from the column faces. The failure of all the tested precast subassemblages was identified as being caused by the significant shear deformation in the plastic hinge regions;

2. All the frames could be loaded to a DF of at least 3. All these values proved the possession of the limited ductility behavior. In terms of strength, it is evident that the flexural strength capacity can be maintained to levels at an interstory drift beyond 2.5%. The energy dissipation characteristic was also satisfactory. Hence, the subassemblages incorporating the relocated connections reported in this paper are appropriate in providing sufficient seismic resistance in areas of low-to-moderate seismicity;

3. It has been noted that the lapping of the hooked bars at the connections began in the vicinity of 1.5d from the column faces, rather than 2d, as required by ACI 318. Generally, the test results have shown that the connections could perform satisfactorily under load reversal. The construction joints between the precast and cast-in-place concrete did not cause a detrimental effect. Nevertheless, greater inelastic tensile strains were recorded at the column face for both the precast units tested. Because only one span-depth ratio has been tested, experimental tests on beams with different span-depth ratios are therefore necessary to establish the confidence needed to placing the connections at 1.5d from the column face; and

4. Based on the test results of Unit 2, significant bond deterioration was observed in the connection regions due to the insufficient anchorage length when 90-degree hooks were used. This premature bond failure was identified as the root cause of stiffness degradation within the entire frame. Therefore, such a connection detail is not recommended for shallow beams. It is believed, however, that a 90-degree hook with increased anchorage length can be used in beams with a greater depth. The connection detail established by overlapping 180-degree hooks is recommended for application

as it has exhibited the closest replication of monolithic structural characteristics in terms of strength, stiffness, ductility, and energy dissipation. Transverse rods of equivalent size are recommended to be placed in contact with the concave side of the hooks to help distribute the bearing stresses acting against the hooks. Sufficient transverse reinforcement must also be provided to transfer the entire shear force entering the connection region.

ACKNOWLEDGMENTS

The research funding provided by the Nanyang Technological University, Singapore, is gratefully acknowledged.

NOTATION

DF	=	displacement ductility factor
d	=	effective beam depth
EI	=	flexural rigidity of section
f_c'	=	cylinder compressive strength of concrete
I_g	=	moment of inertia based on uncracked gross concrete area
K_{Test}	=	measured initial stiffness of test specimen
K_{th}	=	calculated theoretical initial stiffness of test specimen
P_{th}	=	theoretical total lateral load capacity of test specimen
Δ	=	imposed lateral displacement during test
$\Delta_{0.75}$	=	Measured lateral displacement at $0.75P_{th}$
Δ_y	=	measured initial yield displacement of test specimen
ε_y	=	yield strain of steel reinforcing bar
μ_Δ	=	displacement ductility factor in test

REFERENCES

1. Naaman, A. E.; Wight, J. K.; and Abdou, H., "SIFCON Connections for Seismic Resistant Frames," *Concrete International*, V. 9, No. 11, Nov. 1987, pp. 34-39.

2. ICBO, "Uniform Building Code (UBC: 91)," International Conference of Building Officials, Whittier, Calif., 1991, 1050 pp.

3. Priestley, M. J. N., "Seismic Design Philosophy for Precast Concrete Frames," *Journal of Structural Engineering International*, Jan. 1996, pp. 25-31.

4. Lin, C. M.; Restrepo, J. I.; and Park, R., "Seismic Behavior and Design of Reinforced Concrete Interior Beam-Column Joints," *Research Report* 2000-1, Department of Civil Engineering, University of Canterbury, New Zealand, 2000, 471 pp.

5. Park, R., "A Perspective on the Seismic Design of Precast Concrete Structures in New Zealand," *PCI Journal*, V. 40, No. 3, 1995, pp. 40-60.

6. French, C. W.; Amu, O.; and Tarzikhan, C., "Connections between Precast Elements—Failure Outside Connection Region," *Journal of Structural Engineering*, ASCE, V. 115, No. 2, 1989, pp. 316-340.

7. French, C. W.; Hafner, M.; and Jayashankar, V., "Connections between Precast Elements—Failure Within Connection Region," *Journal of Structural Engineering*, ASCE, V. 115, No. 12, 1989, pp. 3171-3192.

8. Restrepo, J. I.; Park, R.; and Buchanan, A. H., "Seismic Behavior of Connections between Precast Concrete Beams," *Research Report 93-3*, Department of Civil Engineering, University of Canterbury, Christchurch, New Zealand, 1993, 380 pp.

9. Restrepo, J. I.; Park, R.; and Buchanan, A. H., "Design of Connections of Earthquake Resisting Precast Reinforced Concrete Perimeter Frames of Buildings," *PCI Journal*, V. 40, No. 5, pp. 68-81.

10. SANZ, "Code of Practice for the Design of Concrete Structures (NZS 3101:1995)," Standards Association of New Zealand, Wellington, 1995, 256 pp.

11. Park, R., "Evaluation of Ductility of Structures and Structural Assemblages from Laboratory Testing," *Bulletin of the New Zealand National Society for the Earthquake Engineering*, V. 22, No. 3, 1989, pp. 156-166.